ARTICLE

Workability and Strength of Ceramsite Self-Compacting Concrete with Steel Slag Sand

Suiwei Pan[1], Anqi Ren[1], Yongli Peng[1], Min Wu[2], Wanguo Dong[3], Chunlin Liu[2] and Depeng Chen[2,*]

[1]School of Construction Engineering, Ma'anshan University, Ma'anshan, 243100, China

[2]School of Architectural and Civil Engineering, Anhui University of Technology, Ma'anshan, 243032, China

[3]School of Management Science and Engineering, Anhui University of Technology, Ma'anshan, 243032, China

[*]Corresponding Author: Depeng Chen. Email: dpchen@ahut.edu.cn

ABSTRACT

This study focuses on the workability and compressive strength of ceramsite self-compacting concrete with fine aggregate partially substituted by steel slag sand (CSLSCC) to prevent the pollution of steel slag in the environment. The SF, J-ring, visual stability index, and sieve analysis tests are primarily employed in this research to investigate the workability of freshly mixed self-compacting concrete containing steel slag at various steel slag sand replacement rates. The experiment results indicate that CSLSCC with the 20% volume percentage of steel slag (VPS) performs better workability, higher strength, and higher specific strength. The 7-day compressive strength of CSLSCC with the 0.4 of the water-binder ratio (W/B), decreases with the increase of steel slag content, while the 28-day compressive strength increases significantly. The ceramsite self-compacting concrete with good comprehensive performance can be obtained when the substitution rate of steel slag sand for fine aggregate is less than 20% (volume percentage).

1 Introduction

Concrete is currently the most widely used building material in the world, conventional concrete, also known as normal strength concrete [1], no longer meets the requirements for the execution of these works due to advancements in cement science and technology, as well as the requirement for slender and bolder structures as a result of the advancement of cement science and technology. There have been developments in different concretes and other cementitious mixes that have qualities that outperform conventional concrete. The aggregate, which is the main component of concrete, accounts for roughly 70% of the volume of concrete [2,3]. Sand and gravel are non-renewable resources, and the exploitation and use of natural aggregates seriously damage the ecological environment. The world's annual sand and gravel consumption are increasing year by year, which must be taken seriously to find appropriate alternative resources to reduce the exploitation and use of these non-renewable natural materials, which are sustainable for the construction sector [4]. Steel slag is a main by-product of the steel smelting process, accounting for approximately 10%–15% of total crude steel production [5]. Steel slag

accumulates in large quantities due to its low utilization rate, not only occupying land and polluting the environment but also causing waste of resources. Construction debris or industrial by-products, such as steel slag, slag, tailings, and so on, are examples of solid waste. Because a big amount of waste takes up space, pollutes the environment, and wastes resources, it is impeding the path to sustainable development. In certain cases, researchers suggest using agroindustrial leftovers or byproducts instead of clinker. This is true of slag, fly ash, silica fume, and various pozzolans, such as agricultural ashes. Reduced usage of clinker, which is often more expensive than aggregates, reduced manufacturing costs [6].

To reduce the amount of natural sand and gravel used in construction, researchers have tried to investigate the possibility and effect of steel slag used to replace powder [7–10] or aggregate [11–14] components in concrete [15–17], and some positive effect of using steel slag on the performance of ordinary concrete were reported [18,19]. According to the research of Qiang et. al. [20], In steel slag powder can reduce the heat of hydration of concrete and improve its fluidity, and granular steel slag can increase the strength of concrete [21,22], and improve its mechanical properties. For the past 40 years, concrete has been obscurely "eating" powder and "swallowing" slag, making an essential contribution to the sustainable development of the construction field. With the advent of self-compacting concrete (SCC), scholars from various countries have begun to study the application of slag in self-compacting concrete [23,24]. It has the advantages of ordinary self-compacting concrete without vibration, good flow performance, low construction noise, and so on because of its lightweight, higher specific strength, good heat preservation, moisture retention, excellent seismic performance, and better fire resistance. Concrete development has become an essential direction due to several advantages [25]. Sheen et al. [24] and others studied stainless steel oxide slag (SSOS, partly replacing natural aggregates) and stainless steel reduced slag (SSRS, partly replacing cement) to produce self-compacting concrete. The test results show that when no more than 20% of SSRS replaces OPC, the slump gradually increases; The T500 and V-shaped funnel of SSRS-based fresh SCC is prolonged. At the same time, the SSOS-based self-compacting concrete can be beneficial to the hardening process, and the compressive strength of the self-compacting concrete prepared after completely replacing the SSOS is slightly better, or similar, but there is potential volume instability. Santamaria et al. [26,27] studied the influence of electric arc furnace slag (EAFS) on the performance of self-compacting concrete, prepared self-compacting concrete with EAFS as aggregate, tested its fresh mixing performance and hardening performance, and concluded that EAFS could be used. The slag is coarse and fine aggregates. Use appropriate dosage and compatible chemical additives to prepare SCC.

Hisham [28] studied the influence of steel slag instead of natural aggregate on self-compacting concrete, and used SF test, V-funnel test, U-box test, sedimentation column test, and sieve analysis test. The results show that the SS can be used as aggregate to prepare self-compacting concrete, but when the replacement rate of steel slag exceeds 50%, it has a significant impact on the performance of SCC. Rehman et al. [29] studied the preparation of SCC by replacing cement with glass powder and fine aggregate with granular steel slag (GSS) and studied its mechanical properties and workability. It turns out to be the case that the workability of self-compacting concrete decreases with risen the GSS content. Analysis suggests that this might be related to the porous and rough structure of the slag, while the strength of the GSS increases with risen the granulated slag content. Pan et al. [7] studied the effect of SSP on the properties of recycled aggregate SCC, and the results have shown that SSP could improve the filling ability and passability of self-compacting concrete. However, it has hurt the anti-segregation performance. Based on rheology and physical mechanics experiments, Sosa et al. [30] studied the use of EAFS as aggregate and added dome slag powder to prepare high-performance SCC. The results show that under the condition of no segregation or no aggregate accumulation, a very uniform, symmetrical, and stable distribution of the mixture can be obtained. When the EAFS substitution rate is 10%, the slump and throughput of concrete are reduced. Due to its high viscosity, EAFS reduces the fluidity more significantly. Khan et al. [31] used

vinyl acetate (EVA) instead of cement, steel slag, and ladle slag (LFS) instead of natural sand to prepare self-compacting concrete. The results show that the addition of EVA is beneficial to the performance of self-compacting concrete, while LFS reduces its performance. Pan et al. [32] used slag instead of natural sand as a fine aggregate to explore the effect on the performance of SCC. The results showed that with the increase of fine slag, the flow performance and interstitial passability of self-compacting concrete decreased. When the slag content is 20%, the workability is the best. Azevedo et al. [33] looked into the use of construction waste (CDW) to replace natural sand in mortar. They found that when the CDW substitution rate is more than 25%, the mortar water demand is higher. The rate at which the mortar can take in water increases as the CDW increases. The recommended replacement rate should not be more than 25%.

The use of industrial waste as a substitute for cement or natural aggregates not only reduces land occupation and air pollution but also reduces the development of natural resources, which is extremely important [34,35]. Although many scholars have studied and explored the application of steel slag to concrete and self-compacting concrete [23,27] the high water absorption rate of slag is not conducive to the flow capacity of fresh concrete. Of course, other than that. Steel slag has also been used in other related studies [36–39]. To a certain extent, research work on steel slag has just begun in recent years. Moreover, there are relatively a few articles on the use of slag on lightweight aggregate self-compacting concrete (LSCC). Furthermore, encouraging the usage of steel slag without any reservations or worries is insufficient if the technical judgments are not backed up by suitable characterization and performance testing. Therefore, this article focuses on using granular steel slag as aggregate, and the aged slag added to LSCC to study its effect on the performance of concrete. The workability of CSLSCC is systematically analyzed by studying the workability of freshly mixed LSCC to promote the widespread use of granular steel slag in LSCC and to promote the conservation and long-term development of traditional materials. It is of great significance.

2 Materials and Methods

2.1 Materials

2.1.1 Cement

Since SCC has no special requirements for cementitious materials, P.O.42.5 ordinary Portland cement supplied by Anhui Conch Co., Ltd. (Anhui, China) is used. The specific performance indicators are shown in Tables 1 and 2.

Table 1: Chemical composition of cement and fly ash (%)

Constituent	SiO_2	CaO	MgO	Al_2O_3	SO_3	Fe_2O_3	Others
Cement	20.52	59.65	2.58	5.95	2.47	2.75	6.08
Fly ash	52.7	3.7	1.2	25.8	0.2	9.7	6.7

Table 2: Basic properties of cement

Cement fineness/(m^2/kg)	Initial setting time/min	Final setting time/min	Compressive strength /MPa	
			3 d	28 d
350	60	280	24.5	49.0

2.1.2 Coarse Aggregates

Ceramsite with a particle size of 5–16 mm was used in this experiment as the coarse aggregate particle size. Ceramsite absorbs more water than conventional sand and stone, which will have a stronger influence on workability. The water absorption of ceramsite was measured before using it as aggregate in the experiment. The ratio of the amount of water absorbed by ceramsite to the weight of dry material is referred to as water absorption. Take 1200 g of the dried ceramsite used in the test and measure the 96-h water absorption rate. The test results are shown in Table 3 and Fig. 1.

Table 3: Water absorption of ceramsite

Time/h	0	0.25	0.5	1	2	4	8	12	24	48	96
Water absorption/%	0	8	10	11	12	14	15	16	17	17.4	17.4
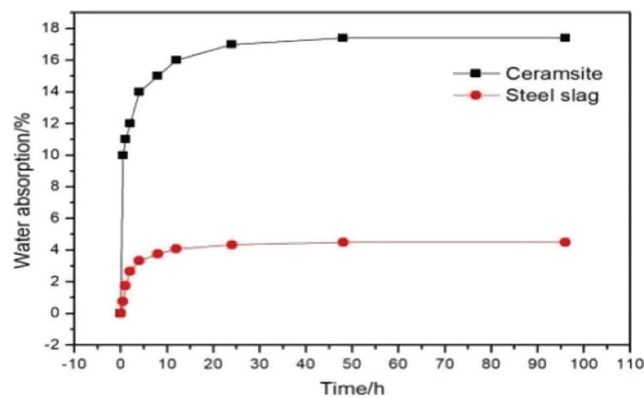
Figure 1: The relationship curve between water absorption of ceramsite and time

2.1.3 Natural Fine Aggregates

The fine aggregate used is ordinary river sand with a fineness modulus of 2.4, which belongs to the middle sand in Zone-II according to *Sand for Construction* (GB/T 14684-2011). The fineness modulus and mud content of fine aggregate are the most important test indications. The river sand with a mud content of 1.2%, water content of 2.8%, and bulk density of 1560 kg/m^3 was used, which meets the requirements of ordinary concrete with the strength grade of C30~C60.

The natural fine aggregate grading curve, using the cumulative percentage of sieve residue as the ordinate and the sieve size as the abscissa, is illustrated in Fig. 2.

2.1.4 Steel Slag Sand

Steel slag particles that had been deposited for a long time in a steel plant in Anhui Province were used in the experiment. Steel slag replaces natural sand as fine aggregate. It uses the current industry standard *Quality Standards and Inspection Methods of Sand and Stone for Common Concrete for Sampling and Testing* (JGJ 52-2006). The chemical composition of steel slag sand tested by XRD diffraction is shown in Table 4.
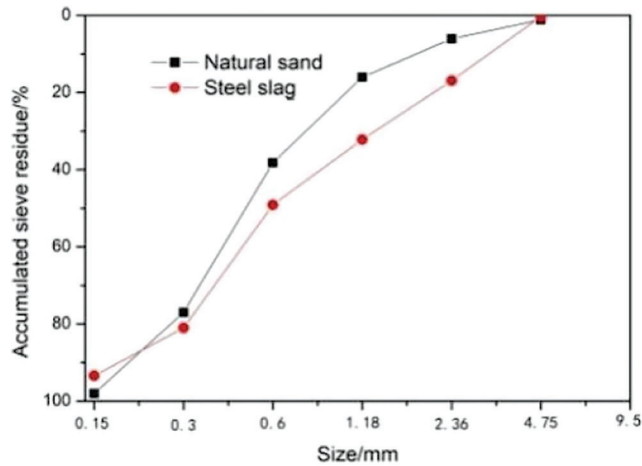
Figure 2: Granulometriccurve of natural sand and steel slag

Table 4: Chemical composition of steel slag

Chemical composition	CaO	SiO_2	Fe_2O_3	P_2O_5	Al_2O_3	MgO	MnO	SO_3	Others
Content/%	50.32	12.06	21.40	3.02	1.53	4.05	2.21	0.3	5.11

After data calculation, the result is 2.7, which belongs to the middle sand in a Zone-II and meets the standard sand use regulations. The natural fine aggregate grading curve is illustrated in Fig. 2 using the cumulative percentage of sieve residue as the ordinate and the sieve size as the abscissa. Take out a certain amount of steel slag powder that meets the test conditions for XRD testing, and the results are shown in Fig. 3.
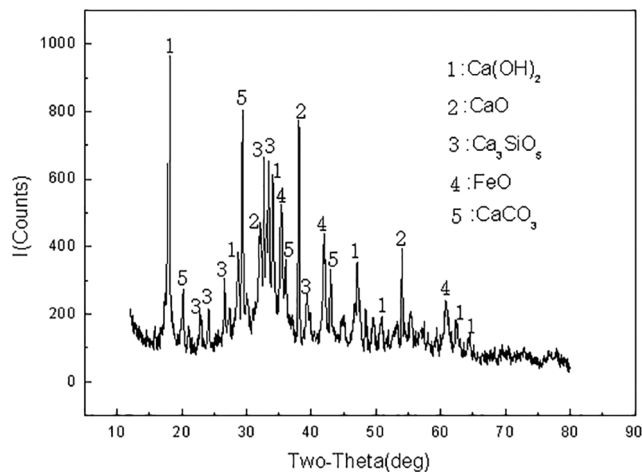

Figure 3: XRD test results of steel slag

Fig. 3 indicates that most of the constituent materials exist in the form of oxides, which are due to the long storage time of steel slag sand. The existence of $Ca(OH)_2$ was revealed by XRD mapping analysis. $Ca(OH)_2$ is produced primarily through the long-term reaction of f-CaO in steel slag with water. $Ca(OH)_2$

improves the concrete's strength, as demonstrated in Fig. 3. CaO has a negative effect on concrete's strength. Steel slag comprises $Ca(OH)_2$ and other components, indicating that the internal f-CaO has undergone hydration, has been stacked for a long period, and has inert performance. Because the surface of GSS is rough and porous, it has better water absorption than ordinary sand and gravel, which will have a more significant impact on the workability of CSLSCC. Consequently, it is necessary to measure the water absorption of steel slag sand before using it in CSLSCC and testing the performance. The water absorption rate refers to the proportion of the water absorption of GSS to the dry weight of the material. Take 1200 g of the dried steel slag sand used to test its water absorption rate. The test results are shown in Table 5 and Fig. 1.

Table 5: Water absorption of steel slag sand

Time/h	0	0.5	1	2	4	8	12	24	48	96
Water absorption/%	0	0.75	1.75	2.67	3.33	3.75	4.08	4.33	4.50	4.50

As shown in Fig. 1, the water absorption rate of steel slag sand increased rapidly in the first 4 h. This has a more significant impact on the workability of CSLSCC, especially the fluidity and segregation resistance of the fresh mixture. Controlling the time from mixing to mold loading should be a priority during the test.

2.1.5 Mineral Admixture

Grade II fly ash, according to *Fly Ash Used for Cement and Concrete* (GB/T 1596-2017), was utilized as an admixture in the experiment. Table 1 shows the chemical composition of fly ash with 460 m^2/kg specific surface area, 2.7×10^3 kg/m^3 density, and 2.04% ignition loss.

2.1.6 Water-Reducer

The polycarboxylic acid series high-performance water-reducer agent produced by a particular building material company in Nanjing was used in the experiment. Its physical properties and dosage are shown in Table 6.

Table 6: physical characteristics and recommended dosage of polycarboxylic acid water reducer

| Admixture state	Solid content/%	pH	Total alkali/%	Suggested dosage/%
Liquid	22 ± 1	6~8	≤2.0	0.8~1.5

2.1.7 Water

According to *Concrete Water Standard* (JGJ 63-2006), tap water was used as the mixing water in the experiment.

2.2 The Benchmark Mix Ratio

Fig. 4 shows the components used in the green high-performance concrete, which is referred to as CSLSCC, prepared with steel slag partially or entirely replacing natural fine aggregate. Compared with ordinary concrete, CSLSCC shows improved fluidity, lower construction costs, and less environmental noise pollution. However, there is currently no common guideline for the mix ratio design of CSLSCC. Many scholars have provided considerable approaches to combining LSCC with SCC mix design based on scientific considerations and experimentation [40–42]. Although, the design method of LSCC mix ratio in the literature is mainly based on the secure aggregate packaging method. This article preliminarily constructs the LSCC mix ratio based on the appropriate specifications and previous experience [43],

intending to design and calculate the mix ratio of steel slag sand pottery self-compacting concrete. Finally, combined with the work performance of steel slag sand ceramic self-compacting concrete, the most reasonable mix ratio is obtained. In general, there are four control parameters for the mixing ratio of SCC: cementitious material, unit water consumption, coarse, and fine aggregates, and admixtures. For CSLSCC, the optimal mix ratio is also obtained by adjusting these control parameters.
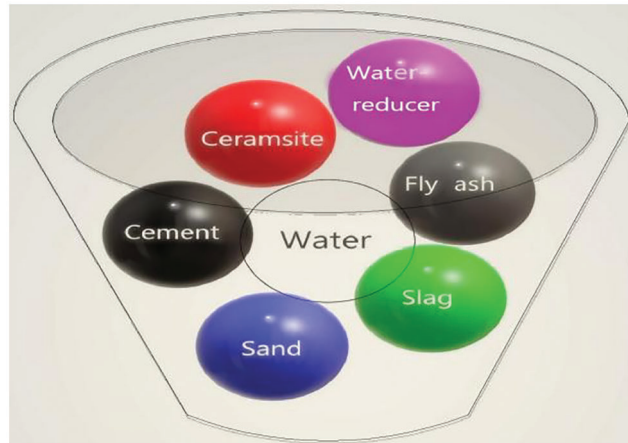
Figure 4: Schematic diagram of CSLSCC composition

In this experiment, the volume percentage of steel slag sand (VPS) is used as a variable parameter; that is, the equivalent volume replacement rate of steel slag sand is 0.0%, 10%, 20%, 30%, 40%, and 50%, and the equivalent volume of slag replaces fine natural aggregate, and ceramsite as coarse aggregate. The materials are tested and compared and analyzed. In each group of specimens, steel slag consumption should be changed to maintain the mix ratio of the steel slag sand to the concrete mix to evaluate the impact of steel slag sand on the work performance and compressive strength of CSLSCC. The preparation of each group is shown in Table 7. Among them: LSCC: ordinary lightweight aggregate self-compacting concrete; LSCC-S_{10}: steel slag sand aggregate equal volume of LSCC instead of 10% natural fine aggregate; LSCC-S_{20}: steel slag sand aggregate equal volume of LSCC instead of 20% natural fine aggregate LSCC; LSCC-S_{30}: LSCC with steel slag sand aggregate equal volume instead of 30% natural fine aggregate; LSCC-S_{40}: LSCC with steel slag sand aggregate equal volume instead of 40% natural fine aggregate; LSCC-S_{50}: steel slag sand aggregate Equivalent volume replaces 50% natural fine aggregate LSCC.

Table 7: Replacement of GSS

Group	Symbol	Detail
1	LSCC	Ordinary lightweight aggregate self-compacting concrete
2	LSCC-S_{10}	Steel slag sand aggregate equal volume instead of 10% fine aggregate
3	LSCC-S_{20}	Steel slag sand aggregate equal volume instead of 20% fine aggregate
4	LSCC-S_{30}	Steel slag sand aggregate equal volume instead of 30% fine aggregate
5	LSCC-S_{40}	Steel slag sand aggregate equal volume instead of 40% fine aggregate
6	LSCC-S_{50}	Steel slag sand aggregate equal volume instead of 50% fine aggregate

2.3 Test Method (Dynamic Stability and Static Stability Method)

Ordinary SCC is wildly used in the construction industry due to its high fluidity, good uniformity, and stability. As this performance of SCC cannot be thoroughly expressed and reflected by a single index or measurement method, its effectiveness cannot be evaluated through a single index or measurement method. In general, workability mainly includes three types of performance indicators: filling ability, passing ability, and segregation resistance. Therefore, the performance evaluation of CSLSCC can be carried out based on the three types of performance indicators, such as filling ability, passing ability, and segregation resistance, which can give a comprehensive assessment of the static stability and the dynamic stability of the material.

Several experimental methods and experimental instruments have been developed to evaluate the performance of SCC. Due to the limitations of testing equipment and time, for the research on the working performance of steel slag sand ceramic self-compacting concrete, this paper adopts SF, T500, and J-ring tests to evaluate the dynamic stability of CSLSCC, and the sieve analysis method and visual stability evaluate the static stability of CSLSCC. Each index's performance is shown in the following Table 8.

Table 8: Workability research methods and test performance

Method type	Evaluation	Evaluation index	Workability
Basic workability	Slump flow test	Slump flow (SF)	Filling ability
	T500 test	Flow time (T500)	Filling ability
	J-ring test	J-ring blocking height difference (Δh)	passing ability
		J-ring Slump flow (SF_J)	passing ability
Static stability performance	Sieve analysis method	Segregation rate (SR)	Segregation resistance ability
Dynamic stability performance	Visual Stability Index (VSI)	Visual Stability index (VSI)	Segregation resistance ability

The slump flow test, as we all know, is one of the relatively simple and effective procedures for evaluating the flowability of SCC by examining three parameters: SF, flow velocity, and T500.

It has been accepted by many researchers since British scholar Bartos et al. [44] proposed the J-ring test to evaluate self-compacting concrete. The J-ring test uses two parameters, namely the J-ring slump flow (SFJ) and the blocking height difference (Δh), to reflect the gap passing capacity of the self-compacting concrete. In accordance with Chinese standards (JGJ/T283-2012) [45], the difference between SFJ and SF is used to evaluate passing ability (PA), categorized into PA1 (25 mm < PA ≤ 50 mm) and PA2 (0 mm ≤ PA ≤ 25 mm). PA1 should be used for structures with a spacing of 80–100 mm. Typically, PA2 is used in structures with steel bar spacing in the range of 60 to 80 mm.

As from 2009, the Visual Stability Index [46] method was incorporated into the American ASTM standard and adopted by the American concrete industry. As part of the method, observers observe the surface condition of the mixture and combine it with standards for evaluation. VSI evaluation criteria are in Table 9.

Table 9: VSI evaluation criteria for self-compacting concrete

Stability level	Evaluation description
0 (good stability)	No obvious segregation or bleeding
1 (General stability)	No obvious segregation, slight bleeding
2 (Poor stability)	A slight halo of mortar or aggregate accumulation
3 (Extremely poor stability)	Obvious segregation occurs and more aggregate accumulation

Note: When there is a slight mortar halo (≤10 mm) in the mixture, the stability is poor; when the mortar halo in the mixture is greater than 10 mm, it belongs to the grade of inferior stability.

Wet Sieve Segregation Tests [47] are commonly used to evaluate anti-segregation in self-compacting mixtures. The degree of segregation risk occurring in time is used to evaluate the static stability performance of the fresh SCC. According to the Chinese Standard JGJ/T 283-2012 "*Technical Regulations for the Application of Self-Compacting Concrete*," the anti-segregation performance of self-compacting concrete is divided into SR1 and SR2. It is classified as SR2 when the segregation index is less than 15%. When the segregation index does not exceed 20%, it is classified as SR1. Among them, SR1 is used for thin plates and vertical structures made up of steel bars spaced apart by 80 mm or more; SR2 is used for thin plates and vertical structures made of steel bars spaced apart by greater than 80 mm and a flow distance of more than 5 m, and SR3 is used for thin plates and vertical structures made up of steel bars spaced apart by 44 to 60 mm.

3 Results and Analysis

3.1 Dynamic Stability of the Benchmark Group of CSLSCC

After experimental analysis, calculations, and adjustments, CSLSCC benchmark coordination such as Table 10 was designed. All of the working indexes in the test meet the specifications. The specific test results are shown in Table 11.

Table 10: Optimization design of benchmark mix ratio of steel slag sand ceramic self-compacting concrete

Group	W/B	W(kg/m^3)	C/(kg/m^3)	MA/(kg/m^3)	G/(kg/m^3)	NS/(kg/m^3)	A/(kg/m^3)
LSCC	0.40	200	350	150	528	636.0	6.36

Table 11: Workability and compressive strength test results of steel slag sand ceramic self-compacting concrete benchmark mix ratio

SF	T500	J-test		Bleeding condition	Installation mode	Stratification situation	7 d strength	28 d strength
		PA	Δh					
710 mm	3.2 s	10 mm	12 mm	No	Fine	Fine	33.6 MPa	38.4 MPa

From Fig. 5 and Table 11, the dynamic performance of the CSLSCC benchmark group is obtained: the SF of the fresh concrete is 710 mm, which belongs to the SF2 grade, indicating that the fluidity of the mixture is better, and its T500 = 3.2 s, in 3 s Within the range of 25 s, meet the target requirements; the PA of the fresh concrete is 10 mm, which meets the PA1 level category, the internal and external height difference is 12 mm, which meets the range of 0~25 mm; the CSLSCC benchmark group has no bleeding or delamination phenomenon, and the mold installation performance is satisfactory. Upon examining the concrete strength after hardening, it appears that the early strength is higher, primarily due to the polycarboxylic acid

water-reducing agent used in this experiment, which significantly increases the early strength by 150%–200%, while the late strength appears to develop slowly. However, the 28 d strength has reached the C35 concrete strength requirement. Test phenomena and data reveal that: under this mix ratio, the CSLSCC's various index parameters comply with the construction and specification standards and meet the pre-set requirements.

(a)   (b)

Figure 5: Test process of steel slag sand ceramic self-compacting concrete benchmark group: (a) SF test and (b) J-test

3.2 Dynamic Stability of CSLSCC with Different VPS

It is possible to divide the performance of steel slag sand ceramic self-compacting concrete into dynamic stability and static stability. SF, T500, and J-ring tests are the characterization of the dynamic stability of CSLSCC. When designing the mix ratio for the dynamic stability test of steel slag sand ceramic self-compacting concrete, VPS is used as a variable parameter, namely 0.0%, 10%, 20%, 30%, 40%, and 50%. Among them, VPS is 0.0%, which is the benchmark mix ratio of steel slag sand ceramics self-compacting concrete. The mixing ratio of each group of CSLSCC in the preliminary design is shown in Table 12.

Table 12: Test mix ratio of each group under different content of steel slag sand

Group	W/B	W/(kg/m^3)	C/ (kg/m^3)	MA/ (kg/m^3)	G/ (kg/m^3)	NS/ (kg/m^3)	SS/ (kg/m^3)	A/ (kg/m^3)
LSCC	0.40	200	350	150	528	626.0	0.0	6.0
LSCC-S$_{10}$	0.40	200	350	150	528	536.4	134.6	6.0
LSCC-S$_{20}$	0.40	200	350	150	528	500.8	140.8	6.0
LSCC-S$_{30}$	0.40	200	350	150	528	438.2	211.3	6.0
LSCC-S$_{40}$	0.40	200	350	150	528	375.6	281.7	6.0
LSCC-S$_{50}$	0.40	200	350	150	528	313.0	352.1	6.0

Note: W/B means water-binder ratio; W means test water consumption; C means test cement consumption; MA means mineral mixture (fly ash); NS means natural sand; SS means steel slag sand; G represents coarse aggregate: A represents water reducer. In the test, considering the water absorption of steel slag sand, it may be difficult to mix during preparation, and the water demand is relatively great. Therefore, when adding steel slag sand aggregate, attention should be paid to the mixing method and mixing time.

After test records, sorting, and analysis, the results of the dynamic stability test (SF test) of CSLSCC are shown in Table 13.

Table 13: Results of dynamic stability test (Slump flow test and J-ring test)

Group	T500/s	SF/mm	PA/mm	Δh/mm
LSCC	3.2	710	10	12
LSCC-S$_{10}$	6.2	705	25	18
LSCC-S$_{20}$	13.5	540	/	/
LSCC-S$_{30}$	/	465	/	/
LSCC-S$_{40}$	/	/	/	/
LSCC-S$_{50}$	/	/	/	/

Note: PA is the difference between SF and SF$_J$, when 0 mm ≤ PA ≤ 25 mm belongs to PA2 grade, when 25 mm < PA ≤ 50 mm belongs to PA1 grade, Δh is the height difference of J-ring blocking, that is when the mixture passes through J-ring, The difference between the inner and outer heights of the J-ring in a static state is generally 0 mm ≤ Δh ≤ 25 mm.

When the VPS gradually increases, as shown in Table 13 and Fig. 6, the mixture gradually thickens. While the T500 increases, the SF value decreases significantly. When the volume percentage of GSS is 10%, its T500 is 6.2 s and the slump flow is 705 mm, which is roughly similar to the LSCC slump flow of 700 mm, which meets the test target requirements. This may be because the VPS is too small and the better combination of particle gradation and natural sand gradation. Therefore, when the VPS is 10%, the filling performance of CSLSCC is similar to that of LSCC. The T500 increases from 3.2 to 13.5 s when the VPS is not less than 20%, while the slump flow of the mixture gradually decreases with the addition of steel slag from 710 to 465 mm. When the VPS is 20%, although the T500 meets the requirements, the final SF value is only 540 mm, which may be considered unsafe according to construction standards. It can be attributed to both the high water requirement and the high viscosity of the mixture, which resulted in fresh concrete that did not meet the test standards in the end. Therefore, the subsequent tests of slump flow and J-rings test with VPS of 30%, 40%, and 50% were not performed according to the original mix ratio.
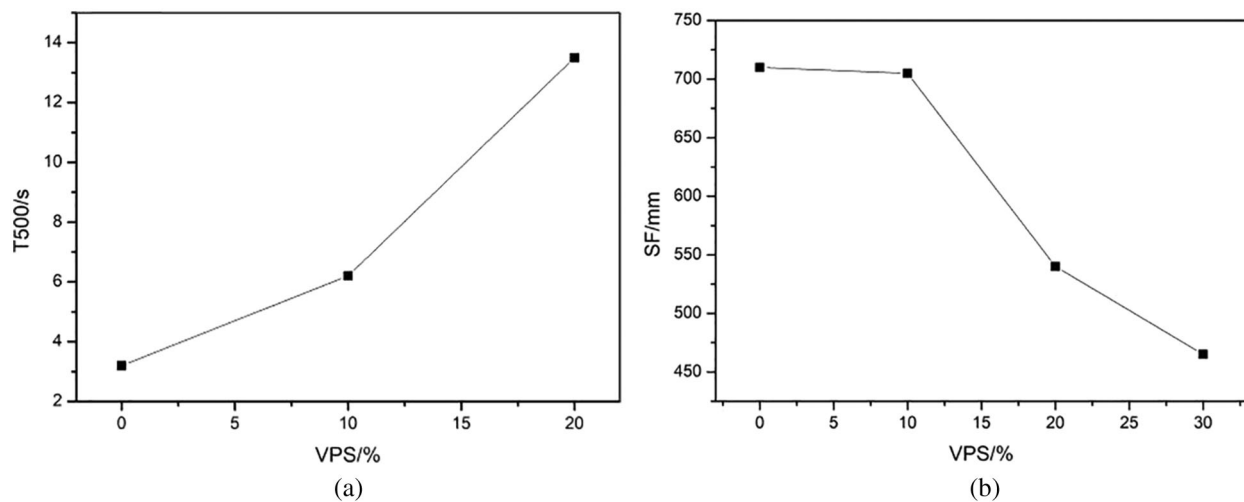

Figure 6: The effect of VPS on T500 (a) and Slump flow (b)

Table 13 shows that as the amount of steel slag increases, the PA and the Δh gradually increase. When the VPS is 10%, the PA is 25 mm, which belongs to the PA2 level. Δh is 18 mm, which meets the test target. It demonstrates that with this mix ratio, the viscosity and fluidity of the steel slag sand ceramsite

self-compacting concrete are better, and the mutual influence is modest. However, when the VPS is gradually increased, the viscosity of the fresh CSLSCC increases, and the influence on its fluidity increases [27]. This result is consistent with previous studies [28,29,32], it's the self-compacting ability decreases as the steel slag increases, which may be related to the porosity and rough structure of the steel slag [29]. It may be that the viscosity increases as the amount of steel slag sand increases. Under the same mixing ratio, the amount of steel slag sand directly affects the existence of free water for flow in the fresh CSLSCC. By reducing the flow performance and reducing the passing workability of the fresh CSLSCC, the relative amount of free water in the mixture decreases. Therefore, the Δh gradually increases.

3.3 Dynamic Stability of CSLSCC with the Optimal Mix Ratio

In the test of CSLSCC under different steel slag sand contents, it is demonstrated that under the same conditions, when the content of steel slag sand is gradually increased, the workability of the fresh LSCC gradually deteriorates to the point of being unusable. When the VPS is 20%, although the fluidity is relatively low, its SF is small, causing the fresh mixture to no longer meet the test target requirements. After that, based on the influence of the steel slag sand content on the CSLSCC benchmark group test, the test group used 20%, 30%, 40%, and 50% of the VPS in the test group by adjusting the slurry-to-bone ratio, the amount of water-reducing agent, and the sand ratio, to test the workability of fresh CSLSCC with different steel slag sand content and conduct experimental research. After continuously changing the composition ratio of the raw materials in the freshly mixed self-compacting concrete, a steel slag sand ceramic self-compacting concrete mix ratio with good workability at various replacement rates is finally obtained. See Table 14 for details.

Table 14: CSLSCC fits well with different steel slag sand replacement ratios

Group	W/C	W/ (kg/m^3)	C/ (kg/m^3)	MA/ (kg /m^3)	G/ (kg/m^3)	NS/ (kg/m^3)	SS/ (kg/m^3)	A/ (kg/m^3)
LSCC	0.40	200	350	150	528	626.0	0.0	6.00
LSCC-S_{10}	0.40	200	350	150	528	536.4	134.6	6.00
LSCC-S_{20}	0.40	202	364	156	528	500.8	140.8	7.80
LSCC-S_{30}	0.40	202	364	156	528	438.2	211.3	7.80
LSCC-S_{40}	0.40	212	371	159	528	375.6	281.7	9.54
LSCC-S_{50}	0.40	212	371	159	500	313.0	352.1	9.54

After the test, the test results are shown in Table 15 and Fig. 7.

Table 15: Results of dynamic stability test (Slump flow test and J-ring test)

Group	T500/s	SF/mm	PA/mm	Δh/mm
LSCC	3.2	710	10	12
LSCC-S_{10}	6.2	705	25	18
LSCC-S_{20}	9.2	680	30	16
LSCC-S_{30}	10.4	710	30	20
LSCC-S_{40}	11.8	700	20	25
LSCC-S_{50}	17.6	685	30	28

It was found that, when the VPS is 10%, due to its low content, it has little effect on the dynamic performance of the fresh concrete, and the performance of LSCC-S_{10} is similar to the benchmark group LSCC. When the VPS is 20%, 30%, or 40%, but by adjusting the number of raw materials, it is possible to try out the CSLSCC that works well and meets the specifications. However, when the replacement rate of steel slag sand is 50%, although the flow of the mixture is the T500 meets the requirements of the specification, the time is longer and has reached 17.6 s. In light of the possibility that self-compacting concrete may be related to certain concealed risks.

(a)   (b)

Figure 7: Test process of steel slag sand ceramic self-compacting concrete after adjustment: SF test (a) and J-ring test (b)
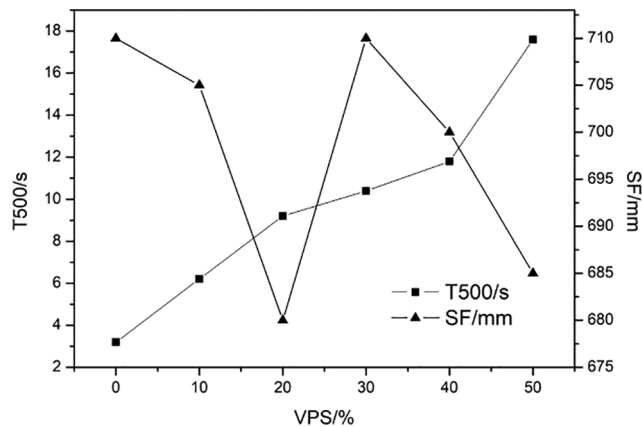
Figure 8: The effect of VPS on T500 and SF after adjustment

From Figs. 8 and 9, it is not difficult to find that various characteristic parameters of the CSLSCC workability under different steel slag content after adjustment meet the expected requirements. The filling ability and passing ability properties of fresh CSLSCC are relatively good, especially when the VPS is 10%, 20%, 30%, or 40%. T500 is less than the specification requirement, and the minimum slump flow is 680 mm, PA max is 30 mm, which meets the standard. The J-ring parameter blocking height difference Δh also meets the requirement of less than 25 mm summarized by experience. When the steel slag sand replacement rate is 50%, although the expected requirements are met, the T500 is relatively long, reaching 17.6 s at the maximum. It may be that when the VPS is large, there is a lack of small aggregate particles in the fine aggregate, and there is no reasonable ground gradation between the mixed fine

aggregates. When the coarse aggregate in the concrete sinks due to its gravity, the mutual resistance between the aggregates increases more, resulting in the average filling performance of fresh CSLSCC. In addition, due to the gradual increase in the amount of slag, the unit water demand gradually increases, resulting in The amount of water used for flow being reduced, so the T500 is longer. Therefore, when using GSS instead of the fine aggregate to test CSLSCC, it is reasonable to suggest that the VPS be no more than 30%.
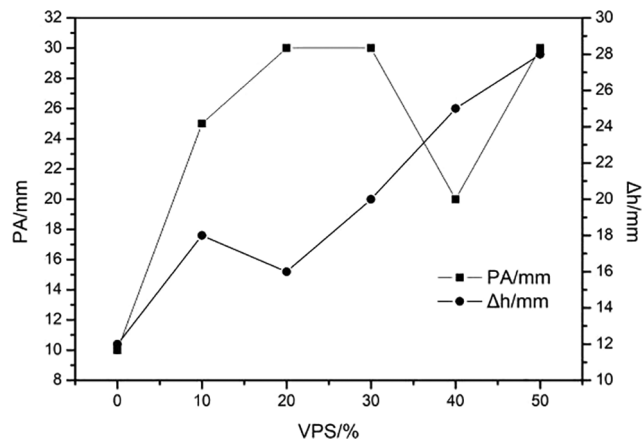
**Figure 9:** The effect of VPS on PA and Δh after adjustment

3.4 Static Stability Test of Steel Slag Sand Ceramic Self-Compacting Concrete

The static stability test of SCC workability is defined in a variety of ways. After generalization, they mainly include static separation column test, sieve analysis test, sinking test, settling column test and visual stability test, etc., aiming at describing the static stability test site of CSLSCC work performance methods. The Visual Stability Index test and the Sieve Segregation Resistance test are used in this article to analyze and assess the static stability (anti-segregation resistance) of SCC at various steel slag sand replacement rates.

3.4.1 Visual Stability Index Method

After testing, it is not hard to figure out that the VSI of CSLSCC with different VPS after the settings were changed all had 0 levels. This means that the performance of stability is better. Results from each group of CSLSCC tests are shown in Fig. 10.

According to the standard, when the performance of the above figures is combined, it can be preliminarily determined that the visual stability index of each test group of steel slag sand ceramic self-compacting concrete is VSI = 0, which means that the static workability (anti-segregation performance) of CSLSCC is essentially equal to or greater than the requirements of the test. VSI is mostly decided by the subjective performance of testers, even though this approach is generally basic and straightforward to assess. Therefore, whether it can meet the requirements of the *"self-compacting concrete pouring construction method"* requires further test verification.
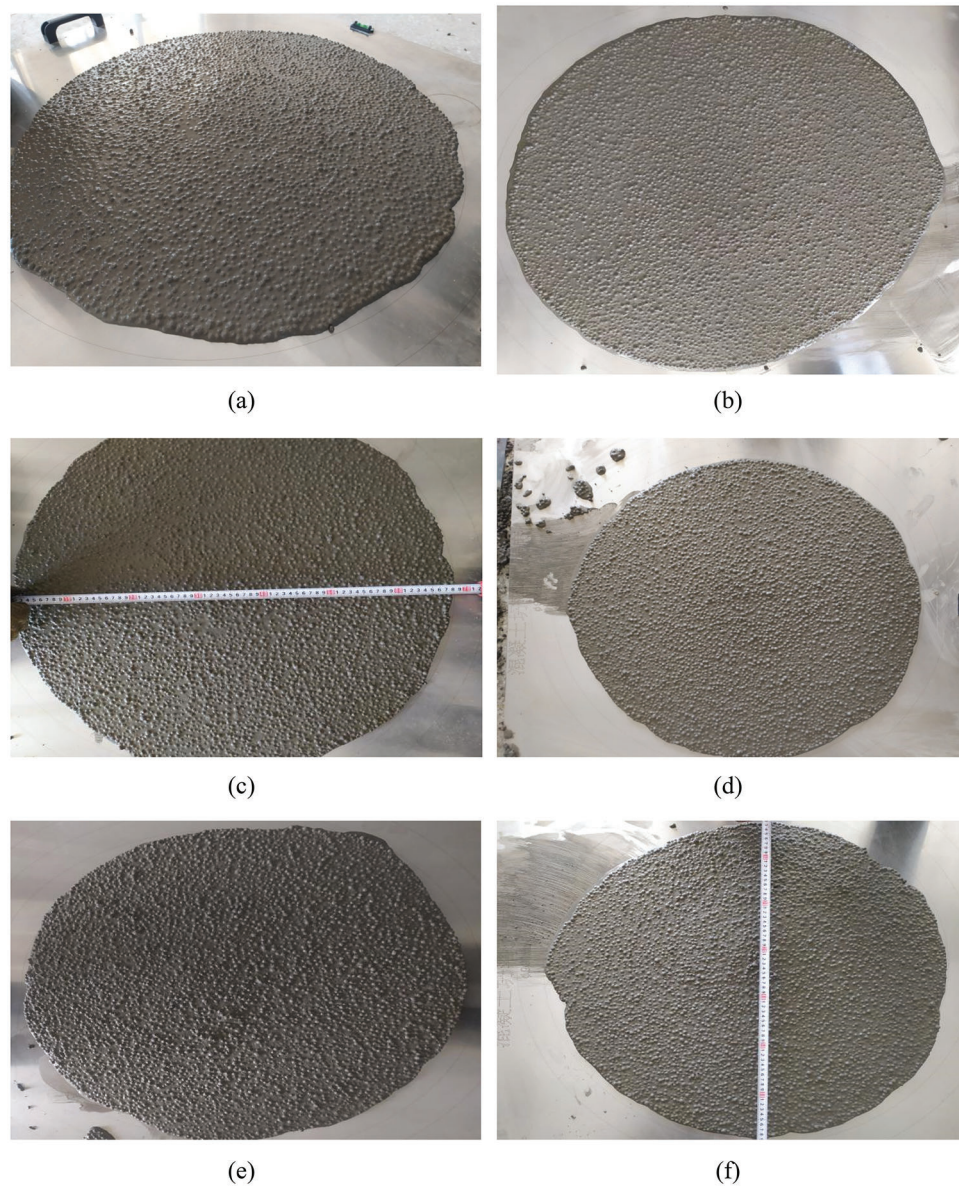
Figure 10: VSI results of each test group of CSLSCC: (a) LSCC; (b) LSCC-S_{10}; (c) LSCC-S_{20}; (d) LSCC-S_{30}; (e) LSCC-S_{40}; (f) LSCC-S_{50}

3.4.2 Sieve Analysis Test

The sieve analysis test process of steel slag sand pottery self-compacting concrete is shown in Fig. 11. The test results of each group of CSLSCC under different steel slag sand content are shown in Table 16 and Fig. 12.

In each group of steel slag sand ceramic self-compacting concrete tests, the sieve analysis results are all less than SR1, that is, less than 15%, which indicates that the test mix ratio used in the concrete has better anti-segregation performance, as shown in Table 16. It is not difficult to find from Table 16 and Fig. 12 that as the VPS continues to increase, the sieve analysis test index SR has a fluctuating trend, with greater dispersion and no apparent regularity, but the overall trend is increasing. When SMT = 30.0%, the SR value is the

largest, and the test result is 1.98%; when SMT = 10.0%, the SR value is the smallest. There is no segregation in the adjusted test mix ratio. Upon examining the experimental results, the SR is generally low as expected due to the relatively large water absorption capacity of ceramsite and steel slag in the early phase. This causes a relative reduction of free water in the mixture, leading to a relatively small segregation rate.

(a)   (b)

(c)   (d)
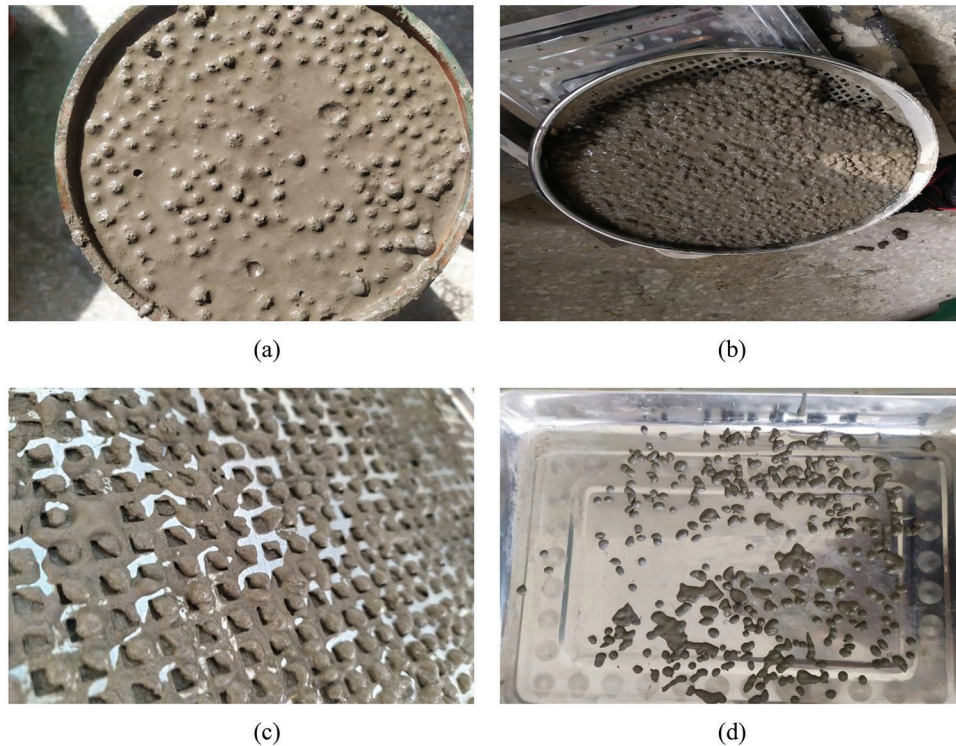
Figure 11: CSLSCC sieve analysis test

Table 16: CSLSCC sieve analysis test results

Group	M_0/kg	M_c/kg	SR/%
LSCC	4.960	0.052	1.05
LSCC-S_{10}	5.010	0.040	0.80
LSCC-S_{20}	5.150	0.060	1.17
LSCC-S_{30}	5.050	0.100	1.98
LSCC-S_{40}	5.086	0.080	1.57
LSCC-S_{50}	4.950	0.064	1.29
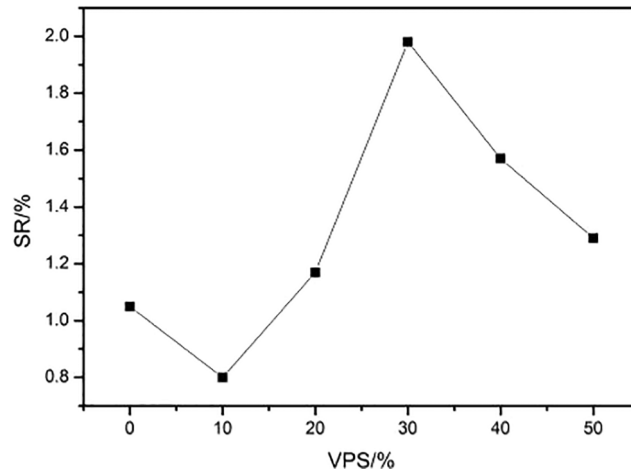
Figure 12: CSLSCC sieve analysis test results of each test group

3.5 Compressive Strength of CSLSCC

3.5.1 Test Basis and Calculation Method

According to *the Standard for Test Methods of Mechanical Properties of Ordinary Concrete* (GB/T 50081-2002) [48], the standard test mold size used for the compressive strength test of ordinary concrete cubes is 150 mm × 150 mm × 150 mm, and it is under standard curing conditions. Dismantle the mold within 24 h. This experiment uses a standard steel test mold with a size of 150 mm × 150 mm × 150 mm. There are no less than 3 test blocks for each group of concrete. The compression strength of cubes aged 7 and 28 d are evaluated under typical curing circumstances. The test findings are summarized once the data has been captured, sorted, and assessed.

According to relevant regulations, the arithmetic average of the strengths of three test blocks should be used to determine the strength representative value for each set of test blocks.
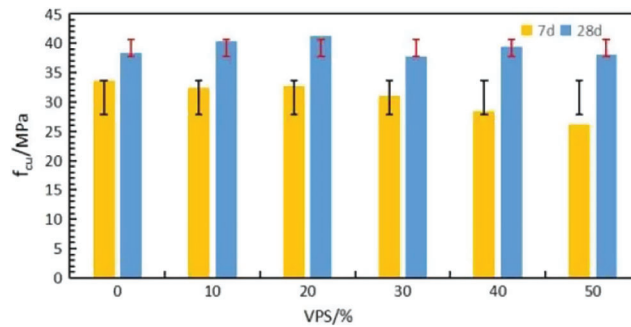
3.5.2 Early Compressive Strength of CSLSCC

After recording and calculation, the curing age of steel slag sand ceramic self-compacting concrete is 7 d and 28 d strength. The results are shown in Table 17.

Table 17: Early compressive strength of the CSLSCC with different content

Group	7 d strength/MPa	28 d strength/MPa
LSCC	33.6	38.4
LSCC-S_{10}	32.4	40.3
LSCC-S_{20}	32.7	41.3
LSCC-S_{30}	31.0	37.7
LSCC-S_{40}	28.5	39.4
LSCC-S_{50}	26.1	38.0

The comparison of the strength of each group of steel slag sand ceramic self-compacting concrete and the reference group concrete is shown in Fig. 13.

Figure 13: The influence of steel slag sand content on compressive strength

From Table 17 and Fig. 13, it is not difficult to conclude that under the condition of good workability of CSLSCC, as slag consumption gradually increases, the early strength (7 d) of steel slag sand ceramic self-compacting concrete gradually decreases. When the VPS is 0 percent and the 7 d compressive strength of each test group is compared, the steel slag sand ceramic self-compacting concrete has the maximum strength, which is 33.6 MPa. Steel slag sand ceramic self-compacting concrete has the best strength at 7 d when the VPS is less than 20%. This may be one of the main reasons why the hydration process in the concrete is slowed down by the mixing amount of steel slag sand under the same water-binder ratio when the CSLSCC works well and the strength of the concrete is reduced. After 28 d of curing, the strength of each test group reached the C35 construction requirement. The CSLSCC test block group had the best strength when the VPS was 20%, reaching 41.3 MPa, which met the strength requirement of C40. When the VPS comes to 20%, the test group has good workability, forming a compact internal structure of concrete and uniform aggregate distribution. When steel slag is used in place of fine aggregate, concrete strength improves [22,49]. As reported by Guo et al. [49] Concrete's strength increases the highest when steel slag is added at a percentage of 20 percent. In concrete, a strong and dense skeleton develops, which is one of the primary reasons for its strength. It can be concluded from the preceding that, as the content of steel slag sand increases, even though the workability of the concrete mixture meets expected requirements, it is not as good as the previous test groups. As a result, a rise in the amount of steel slag sand in concrete is one of the factors contributing to the reduction in concrete strength.

From Fig. 13 that the concrete strength of each test group increases with age and the later strength growth rate of the test group mixed with steel slag sand is greater than that of ordinary LSCC. This may be caused by the particularity of the steel slag sand surface and composition. Because the surface of GSS is relatively rough, it can produce greater bonding force and mechanical bite force between it and cement stone. This is consistent with the theory that 'the strength will increase with the slurry ratio in a certain interval' proposed by Wu et al. [50] in the study of high-strength concrete. In addition, due to the particular composition of steel slag, it is also beneficial to the later strength (28 d strength) of steel slag sand ceramic self-compacting concrete. The early strength of CSLSCC decreases to a certain extent when the VPS is greater than 20%, which may be due to the relative increase in the amount of mortar in the steel slag sand ceramic self-compacting concrete, and the water film thickness around the coarse aggregates interface increases. The water-cement ratio near the large aggregate is relatively large, forming a framework with more pores than the mortar body, and the strength of the transition zone of the aggregate interface is reduced, bringing about low early strength of concrete.

Therefore, through a scanning electron microscope (SEM) test, the pore distribution in the micro-interface of the benchmark group LSCC is relatively uniform, as shown in Fig. 14a. When the replacement level is 20%, the microstructure of the slag-cement slurry interface is shown in Fig. 14b. There is no obvious boundary between the steel slag particles and the cement paste, the microscopic

interface is dense enough, the bonding force between the GSS and the cement stone is relatively fine, and the appearance of ettringite also improves the early strength of concrete. As the content of steel slag increases, more and more free water will accumulate around the steel slag, resulting in lower area density, larger voids, and poorer adhesion, so the strength is relatively poor as shown in Figs. 14c and 14d. Fig. 14d shows that the volume of calcium hydroxide crystals generated by the hydration of f-CaO is larger. This material is bigger as compared to the calcium hydroxide crystals produced by the hydrolysis of cement clinker, and as a consequence, it has a greater expansion force and fracture. As a result, if the VPS is larger than 20 percent, the strength will almost certainly drop. There is a strong correlation between the surface roughness of steel slag particles, the water absorption capacity of steel slag, as well as CSLSCC strength, and the surface roughness of steel slag particles.
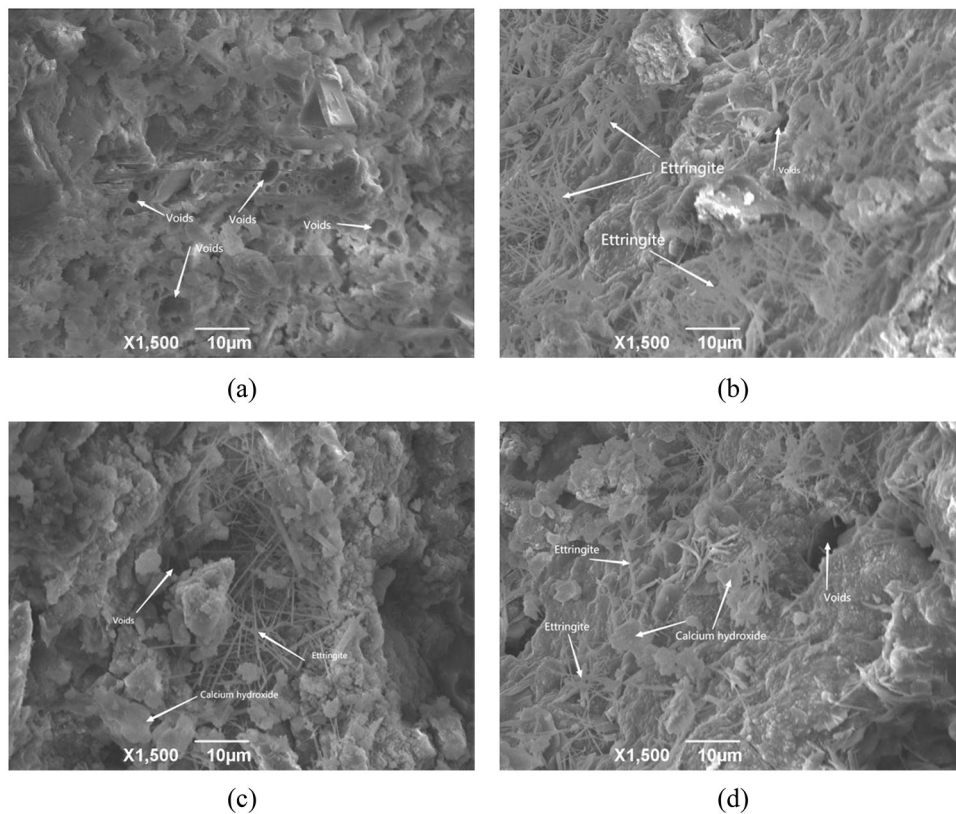
Figure 14: Canning electron microscope pictures: (a) VPS = 0; (b) VPS = 0; (c) VPS = 0; (d) VPS = 0

3.5.3 The Relationship between Dry Density and Strength of CSLSCC

Generally, the apparent dry density of lightweight aggregate self-compacting concrete is less than 1950 kg/m^3, which exhibits the characteristics of lightweight, no need for vibrating, good compaction effect, and excellent uniformity. The quality of CSLSCC varies with the amount of GSS. The specific density grades are shown in Table 18.

Table 18: Density grade of CSLSCC with different content

Group	Density/(kg/m^3)	28 d strength/MPa	Specific strength
LSCC	1830	38.4	0.0210
LSCC-S$_{10}$	1845	40.3	0.0218
LSCC-S$_{20}$	1825	41.3	0.0226
LSCC-S$_{30}$	1890	37.7	0.0199
LSCC-S$_{40}$	1890	39.4	0.0208
LSCC-S$_{50}$	1830	38.0	0.0208

From Table 18 and Fig. 15, it is not difficult to find that when the VPS is 20%, the apparent dry density of the CSLSCC is the smallest. Considering the specific strength, it can be seen that the specific strength of the LSCC-S$_{20}$ group is 0.0226, which is the largest among the experimental groups. With the risen of VPS, the dry apparent density of steel slag sand ceramic self-compacting concrete presents a fluctuating trend that first increases and then decreases. A possible reason for this could be the addition of steel slag, which alters the structure of pores within the concrete and affects the dry apparent density.
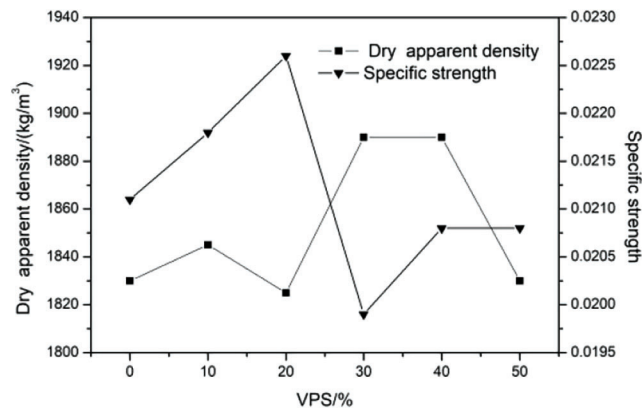
Figure 15: The apparent dry density and specific strength of steel slag sand ceramic self-compacting concrete with different contents

4 Conclusions

In this paper, experimental methods are mainly used to study the workability of freshly mixed CSLSCC under different replacement rates of steel slag sand. The analysis and research are carried out from two perspectives of the dynamic and static stability of freshly mixed CSLSCC. To comprehensively evaluate the workability of freshly mixed self-compacting concrete, various methods such as SF, T500, J-ring, visual stability index method, and sieve analysis test were used and the compressive strength of each group of cubes was determined, and the following results in conclusion were obtained:

(1) With the increase of VPS, the workability of CSLSCC gradually decreases.
(2) According to the results of the dynamic stability test of the workability of the test group, we adjusted the VPS not less than 20% for each group accordingly. By changing the amount of slurry, water-reducer agent, and sand rate, each group with good workability was obtained CSLSCC and met the pre-specified standards.

(3) For the static stability test of the adjusted CSLSCC performance, the visual stability index method and the anti-sieving segregation test are used to comprehensively analyze and assess the results. The results show the anti-segregation ability of each group of adjusted steel slag sand ceramic self-compacting concrete. Relatively good, this complies with the corresponding regulations. It shows that the anti-segregation performance of each experimental group is better.

(4) With the increase of VPS, the strength of CSLSCC gradually decreases after 7 d. However, the 28 d intensity was higher than the baseline group, especially when the VPS was not greater than 20%, and the intensity increased significantly. The steel slag sand content increases, and the steel slag sand ceramic self-compacting concrete strength increases faster in the later stage (before 28 d).

(5) Based on the results of the work performance and strength tests conducted on steel slag sand ceramic self-compacting concrete in each test group, the following recommendations are suggested: when the VPS is not more than 20%, the performance of steel slag sand ceramic self-compacting concrete is relatively good in all aspects.

Conflicts of Interest: The authors declare that they have no conflicts of interest to report regarding the present study.

References

1. Sohail, M. G., Kahraman, R., Alnuaimi, N. A., Gencturk, B., Alnahhal, W. (2020). Durability characteristics of high and ultra-high performance concretes. *Journal of Building Engineering, 33(1–12),* 101669. DOI 10.1016/j.jobe.2020.101669.

2. Al-Jabri, K. S., Hisada, M., Al-Saidy, A. H., Al-Oraimi, S. K. (2009). Performance of high strength concrete made with copper slag as a fine aggregate. *Construction and Building Materials, 23(6),* 2132–2140. DOI 10.1016/j.conbuildmat.2008.12.013.

3. Devi, V. S., Gnanavel, B. K. (2014). Properties of concrete manufactured using steel slag. *Procedia Engineering, 97,* 95–104. DOI 10.1016/j.proeng.2014.12.229.

4. Wei, W., Zhang, W. D., Ma, G. W. (2010). Optimum content of copper slag as a fine aggregate in high strength concrete. *Materials and Design, 31(6),* 2878–2883. DOI 10.1016/j.matdes.2009.12.037.

5. Survey, U. S. G. (2020). *Mineral commodity summaries.* Washington DC, USA.

6. Markssuel, T. M., Afonso, R. G. A., Paulo, R. M., Sergio, N. M., Carlos, M. F. V. (2021). Materials for production of high and ultra-high performance concrete: Review and perspective of possible novel materials. *Materials, 14,* 1–36. DOI 10.3390/ma14154304.

7. Pan, Z. H., Zhou, J. L., Jiang, X., Xu, Y. D., Jin, R. Y. et al. (2019). Investigating the effects of steel slag powder on the properties of self-compacting concrete with recycled aggregates. *Construction and Building Materials, 200(4),* 570–577. DOI 10.1016/j.conbuildmat.2018.12.150.

8. Hu, J. (2017). Comparison between the effects of superfine steel slag and superfine phosphorus slag on the long-term performances and durability of concrete. *Journal of Thermal Analysis & Calorimetry, 128(3),* 1–13. DOI 10.1007/s10973-017-6107-9.

9. Ming, Y., Chen, P., Wang, Y. H., Li, L., Chen, X. D. et al. (2020). Experimental Research of concrete with steel slag powder and zeolite powder. *Journal of Renewable Materials, 8(12),* 1647–1655. DOI 10.32604/jrm.2020.011929.

10. Majhi, R. K., Nayak, A. N., Mukharjee, B. B. (2018). Development of sustainable concrete using recycled coarse aggregate and ground granulated blast furnace slag. *Construction and Building Materials, 159(6),* 417–430. DOI 10.1016/j.conbuildmat.2017.10.118.

11. Xin, Y., Zhong, T., Song, T. Y., Zhu, P. (2016). Performance of concrete made with steel slag and waste glass. *Construction and Building Materials, 114(2),* 737–746. DOI 10.1016/j.conbuildmat.2016.03.217.

12. Palankar, N., Shankar, A., Mithun, B. M. (2016). Durability studies on eco-friendly concrete mixes incorporating steel slag as coarse aggregates. *Journal of Cleaner Production, 129(15),* 437–448. DOI 10.1016/j.jclepro.2016.04.033.

13. Guo, Y. C., Xie, J. H., Zhao, J. B., Zuo, K. X. (2019). Utilization of unprocessed steel slag as fine aggregate in normal-and high-strength concrete. *Construction and Building Materials, 204(2),* 41–49. DOI 10.1016/j.conbuildmat.2019.01.178.

14. Suganya, N., Thirugnanasambandam, S. (2019). Geopolymer concrete using scrap steel slag as coarse aggregate. *International Journal for Research in Applied Science & Engineering Technology, 7(1),* 781–785. DOI 10.22214/ijraset.2019.1122.

15. Rajan, D., Suchithra, S. (2017). Properties of concrete with partial replacement of steel slag with fine aggregate. *Proceedings of the International Conference on Energy, Communication, Data Analytics and Soft Computing*, pp. 3850–3852. Chennai(IN), India.

16. Amaia, S. L., Eduardo, R., Marta, S., Ignacio, M., Javier, J. G. (2016). The use of steelmaking slags and fly ash in structural mortars. *Construction and Building Materials, 106(3),* 364–373. DOI 10.1016/j.conbuildmat.2015.12.121.

17. Nageib, A., Khafaga, M. A., Fahmy, W. S., Hamid, A. M. N. A. (2014). Properties of high strength concrete containing electric arc furnace steel slag aggregate. *Journal of Engineering Sciences, 42(3),* 582–608.

18. Liu, J., Guo, R. H. (2018). Applications of steel slag powder and steel slag aggregate in ultra-high performance concrete. *Advances in Civil Engineering,* 1–8. DOI 10.1155/2018/1426037.

19. Priyanka, S., Shri, S. D., Poovizhi, S. (2017). Experimental investigation on partial replacement of steel slag as coarse aggregate. *Pakistan Journal of Biotechnology, 14(3),* 481–485. DOI 10.1016/j.matpr.2020.09.419.

20. Qiang, W., Yan, P., Mi, G. (2012). Effect of blended steel slag-GBFS mineral admixture on hydration and strength of cement. *Construction and Building Materials, 35(3),* 8–14. DOI 10.1016/j.conbuildmat.2012.02.085.

21. Sezer, G., Güldere, M. (2015). Usage of steel slag in concrete as fine and/or coarse aggregate. *Indian Journal of Engineering and Materials Sciences, 22(3),* 339–344.

22. Saxena, S., Tembhurkar, A. R. (2018). Impact of use of steel slag as coarse aggregate and wastewater on fresh and hardened properties of concrete. *Construction and Building Materials, 165(8),* 126–137. DOI 10.1016/j.conbuildmat.2018.01.030.

23. Yoobanpot, N., Sokrai, P., Makul, N. (2021). Combined recycling of white rice husk ash as cement replacement and metal furnace slag as coarse-aggregate replacement to produce self-consolidating concrete. *Journal of Renewable Materials, 9(11),* 2033–2049. DOI 10.32604/jrm.2021.015849.

24. Sheen, Y. N., Le, D. H., Sun, T. H. (2015). Innovative usages of stainless steel slags in developing self-compacting concrete. *Construction and Building Materials, 101(8),* 268–276. DOI 10.1016/j.conbuildmat.2015.10.079.

25. Uno, Y. (2005). Application of self-consolidating concrete to segment for shield tunnel. *Proceedings of the International Symposium on the Design, Performance and Application of Self-Compacting Concrete*, pp. 665–672. Changsha, China.

26. Santamaria, A., Orbe, A., Losanez, M. M., Skaf, M., Ortega-Lopez, V. et al. (2017). Self-compacting concrete incorporating electric arc-furnace steelmaking slag as aggregate. *Materials and design, 115(7),* 179–193. DOI 10.1016/j.matdes.2016.11.048.

27. Santamaria, A., Ortega-López, V., Skaf, M., Chica, J. A., Manso, J. M. (2019). The study of properties and behavior of self compacting concrete containing Electric Arc Furnace Slag (EAFS) as aggregate. *Ain Shams Engineering Journal, 11(1),* 231–243. DOI 10.1016/j.asej.2019.10.001.

28. Hisham, Q. (2018). Towards sustainable self-compacting concrete: Effect of recycled slag coarse aggregate on the fresh properties of SCC. *Advances in Civil Engineering, 2,* 1–9. DOI 10.1155/2018/7450943.

29. Rehman, S., Iqbal, S., Ali, A. (2018). Combined influence of glass powder and granular steel slag on fresh and mechanical properties of self-compacting concrete. *Construction and Building Materials, 178(30),* 153–160. DOI 10.1016/j.conbuildmat.2018.05.148.

30. Sosa, I., Thomas, C., Polanco, J. A., Setién, J., Tamayo, P. (2020). High performance self-compacting concrete with electric arc furnace slag aggregate and cupola slag powder. *Applied Sciences, 10(3),* 773. DOI 10.3390/app10030773.

31. Khan, K. A., Nasir, H., Alam, M., Khan, S. W., Rehman, Z. U. (2019). Investigation of fresh and hardened characteristics of self-compacting concrete with the incorporation of ethylene vinyl acetate and steel-making slag. *Advances in Civil Engineering, 2(2),* 1–11. DOI 10.1155/2019/9146343.

32. Pan, S. W., Chen, D. P., Ge, G. W., Liu, C. L. (2020). Experimental study on the workability and stability of steel slag self-compacting concrete. *Applied Sciences, 10(4),* 1291. DOI 10.3390/app10041291.

33. Azevedo, A. R. G., Carmo, D., Carmo, D. F., Silva, F. C., Campos, C. M. O. et al. (2020). Analysis of the compactness and properties of the hardened state of mortars with recycling of construction and demolition waste (CDW). *Journal of Materials Research and Technology, 9(3),* 5942–5952. DOI 10.1016/j.jmrt.2020.03.122.

34. Kavyateja, B. V., Jawahar, J. G., Jawahar, C. (2020). Efect of alccofne and fy ash on analytical methods of self-compacting concrete. *Innovative Infrastructure Solutions, 80,* 1–11. DOI 10.1007/s41062-020-00332-9.

35. Saand, A., Ali, K., Kumar, A., Bheel, N., Keerio, M. A. (2021). Efect of metakaolin developed from natural material Soorh on fresh and hardened properties of self-compacting concrete. *Innovative Infrastructure Solutions, 166,* 1–10. DOI 10.1007/s41062-021-00534-9.

36. Shu, Z. Q., Wu, J. M., Chen, S., Yi, S., Li, S. Q. (2022). High-temperature deformation and low-temperature fracture behavior of steel slag rubber asphalt mixture surface layer. *Journal of Renewable Materials, 10(2),* 453–467. DOI 10.32604/jrm.2022.016828.

37. Shu, Z. Q., Wu, J. M., Li, S. Q., Zhang, B. B., Yang, J. Q. (2021). Road performance, thermal conductivity, and temperature distribution of steel slag rubber asphalt surface layer. *Journal of Renewable Materials, 9(2),* 365–380. DOI 10.32604/jrm.2021.014379.

38. Liu, W. H., Li, H., Zhu, H. M., Xu, P. J. (2020). The interfacial adhesion performance and mechanism of a modified asphalt-steel slag aggregate. *Resources Conservation & Recycling, 13,* 1321–1334. DOI 10.3390/ma13051180.

39. Mohamad, A. Y., Jamil, M., Yusoff, N. I., Taha, M. R., Karim, R. et al. (2019). Feasibility study of utilizing steel slag and cathode ray tube glass as aggregate replacement for road base. *International Journal of Nanoelectronics and Materials, 13,* 129–136. DOI 10.3390/ma13051180.

40. Kaffetzakis, M., Papanicolaou, C. (2012). *Mix proportioning method for lightweight aggregate SCC (LWASCC) based on the optimum packing point concept,* pp. 131–151. Netherlands: Springer.

41. Kanadasan, J., Razak, H. A. (2014). Mix design for self-compacting palm oil clinker concrete based on particle packing. *Materials & Design, 56(4),* 9–19. DOI 10.1016/j.matdes.2013.10.086.

42. Li, J., Chen, Y., Wan, C. (2017). A mix-design method for lightweight aggregate self-compacting concrete based on packing and mortar film thickness theories. *Construction & Building Materials, 157(30),* 621–634. DOI 10.1016/j.conbuildmat.2017.09.141.

43. Nepomuceno, M. C. S., Oliveira, L. A., Pereira, S. F. (2018). Mix design of structural lightweight self-compacting concrete incorporating coarse lightweight expanded clay aggregates. *Construction and Building Materials, 166(30),* 373–385. DOI 10.1016/j.conbuildmat.2018.01.161.

44. Bartos, S., Tamimi (2002). *Workability and rheology of fresh concrete: Compendium of tests.* France: RILEM Publications.

45. JGJ/T 283-2012 (2012). Technical specifi<cation for applicaiton of self-compacting concrete. China: China Building Industry Press.

46. Standard, ASTM (2009). Standard test method for slump flow of self-consolidating concrete. USA: ASTM International.

47. The Slef-Compacting European Project Group (2005). The European guidelines for slef-compacting concrete. UK: EFNARC.

48. GB/T 50081-2002 (2002). Standard for test method of mechanical properties on ordinary concrete. China: China Building Industry Press.

49. Guo, Y. C., Xie, J. H., Zheng, W. Y., Li, J. L. (2018). Effects of steel slag as fine aggregate on static and impact behaviours of concrete. *Construction and Building Materials, 192(3),* 194–201. DOI 10.1016/j.conbuildmat.2018.10.129.

50. Wu, J. L., Zhang, R. S., Zhang, L. M., Gao, M. (2001). Study on high-strength and high-performance concrete. *Proceedings of the 4th National Symposium on High Strength and High Performance Concrete and Its Application*, pp. 150–158. Chang Sha, China.